Letter

# Dissipative Dicke time crystals: An atom's point of view

Simon B. Jäger, Jan Mathis Giesen, Imke Schneider, and Sebastian Eggert
*Physics Department and Research Center OPTIMAS, University of Kaiserslautern-Landau, D-67663 Kaiserslautern, Germany*

(Received 9 October 2023; revised 4 April 2024; accepted 21 June 2024; published 18 July 2024)

We develop and study an atom-only description of the Dicke model with time-periodic couplings between atoms and a dissipative cavity mode. The cavity mode is eliminated, giving rise to effective atom-atom interactions and dissipation. We use this effective description to analyze the dynamics of the atoms that undergo a transition to a dynamical superradiant phase with macroscopic coherences in the atomic medium and the light field. Using Floquet theory in combination with the atom-only description we provide a precise determination of the phase boundaries and of the dynamical response of the atoms. From this we can predict the existence of dissipative time crystals that show a subharmonic response with respect to the driving frequency. We show that the atom-only theory can describe the relaxation into such a dissipative time crystal and that the damping rate can be understood in terms of a cooling mechanism.

DOI: 10.1103/PhysRevA.110.L010202

Time-periodic driving of quantum systems allows for the creation of tailored out-of-equilibrium structures including quantum states with topological order [1,2] and self-organized coherent patterns [3–9]. Here, one distinguishes between off-resonant driving and resonant driving. In the high-frequency limit, the former results in a quasistatic quantum system that experiences an engineerable and time-averaged Hamiltonian [10,11]. Resonant driving, instead, enables strong dynamical coherences between otherwise weakly coupled quantum states which can force the quantum system in exotic spatiotemporal patterns. This is exciting as it allows the controlled, on-demand generation of purpose-oriented quantum states but comes at the cost of dealing with an energetically open system, which requires a full understanding of relaxation and decoherence mechanisms to avoid heating by using engineered dissipation [12,13]. Such active *open system control* is in fact one of the main challenges for technological progress in the design of quantum matter. While the Lindblad formalism works well for photonic systems, the description of dissipation in condensed matter with massive particles is often fitted by phenomenological models, with limited understanding and tunability.

We now want to analyze a strongly correlated model of atoms where dissipation is derived microscopically from the interactions with the environment in order to pave the way for quantum state engineering far from equilibrium. For the dissipative Dicke model significant progress has been made to eliminate the cavity in order to derive an effective atom-only master equation [14,15] which is of Lindblad form [16], i.e., the relaxation is directly linked to the interactions of the atoms with photons. However, it is so far unclear if this derivation is valid for time-dependent or periodically driven systems, which are far from equilibrium where the dissipation of large amounts of energy is required. We will derive the atom-only description for the time-periodic dissipative Dicke model which is of large fundamental and prototypical interest. Here, resonant periodic driving can induce the formation of subharmonic spatiotemporal patterns, a so-called dissipative time crystal (DTC). This phase is accompanied by superradiant light emission into the cavity and was recently the focus of several experimental and theoretical works [13,17–24].

Photon elimination is highly nontrivial in this case [25–27] since a strong coupling to the cavity is crucial for two separate mechanisms [28–30]: (i) It mediates tunable time-periodic atom-atom interactions which are essential for the pattern formation via parametric driving [17,31–33]. (ii) The cavity generates dissipation that is required for stabilizing the emerging patterns. In the limit of strong atom-photon interaction the usual approach is therefore to treat the dynamics of atoms and cavity on equal footing.

As we demonstrate in this Letter, the elimination of photons is nonetheless possible and highly successful in the prediction of the full time evolution and the nonequilibrium phase diagram, underlining the advantages of an atom-only description. Analytic predictions of the lower stability threshold and a full analysis of the spectral features and gaps are now possible, hence paving the way for future engineering of tailored dynamic atomic models, which can be used as quantum simulators of complicated interacting systems.

*Model*. We consider the time-periodic dissipative Dicke model and eliminate the cavity in order to derive an effective atom-only master equation which is of Lindblad form [16]. The dynamics of the density operator $\hat{\rho}$ describing the atoms and one coupled cavity mode with loss rate $\kappa$ is governed by the master equation ($\hbar = 1$)

$$\frac{\partial \hat{\rho}}{\partial t} = -i[\hat{H}, \hat{\rho}] - \kappa(\hat{a}^\dagger \hat{a}\hat{\rho} + \hat{\rho}\hat{a}^\dagger \hat{a} - 2\hat{a}\hat{\rho}\hat{a}^\dagger). \tag{1}$$

The coupling to $N$ two-level atoms that are driven by an external laser is described by the Hamiltonian [34–36]

$$\hat{H} = \delta_c \hat{a}^\dagger \hat{a} + \Delta \hat{n}_\uparrow + \frac{g(t)}{\sqrt{N}}(\hat{a} + \hat{a}^\dagger)(\hat{b}_\uparrow^\dagger \hat{b}_\downarrow + \hat{b}_\downarrow^\dagger \hat{b}_\uparrow), \tag{2}$$

where $\delta_c$ is the detuning between the cavity resonance and the external laser drive, $\hat{a}^\dagger$ and $\hat{a}$ are the cavity field creation and annihilation operators, and the product of bosonic operators

 

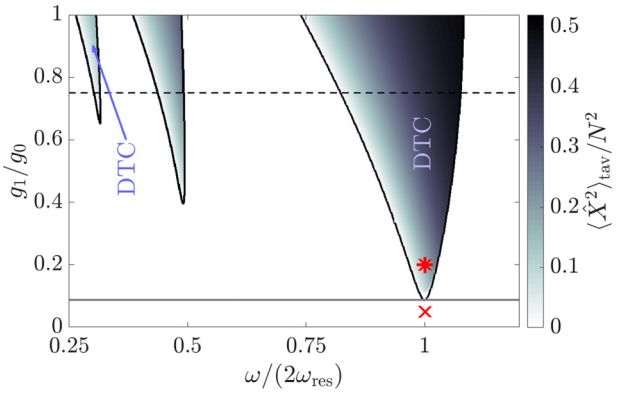


FIG. 1. Time-averaged superradiance order parameter $\langle\hat{X}^2\rangle_{\rm tav}$ calculated from the mean-field Eqs. (8) and (9) and evaluated at $\kappa t = 10^4$ as a function of the driving frequency $\omega/(2\omega_{\rm res})$ and modulation strength $g_1/g_0$. Solid lines mark the threshold to superradiance found by $\gamma_{\rm max} = 0$. The horizontal gray solid line indicates the threshold $g_1^c/g_0$ given by Eq. (12). The red cross ($g_1 = 0.05g_0$, $\omega = 2\omega_{\rm res}$) and star ($g_1 = 0.2g_0$, $\omega = 2\omega_{\rm res}$) correspond to the parameters used in Figs. 2(a) and 2(b), respectively. The dashed horizontal line shows the parameters visible in Fig. 3, $g_1 = 0.75g_0$. We used $\delta_c = \kappa$, $\Delta = 0.1\kappa$, $g_0 = 0.5g_c$. DTC indicates where superradiant phases with subharmonic responses are found.

$\hat{b}_\uparrow^\dagger\hat{b}_\downarrow$ change one atomic state from the ground state $|\downarrow\rangle$ to the metastable excited state $|\uparrow\rangle$ of energy $\Delta$. The operators $\hat{n}_\uparrow = \hat{b}_\uparrow^\dagger\hat{b}_\uparrow$ and $\hat{n}_\downarrow = \hat{b}_\downarrow^\dagger\hat{b}_\downarrow$ measure the number of atoms in each state such that $N = \hat{n}_\uparrow + \hat{n}_\downarrow$. A modulation of the external driving laser leads to a time-periodic collective coupling $g(t) = g_0 + g_1\cos\omega t$, corresponding to two sidebands of the drive.

In the static limit, $g_1 = 0$, the dissipative Dicke model [Eq. (1)] shows a transition from a normal state to superradiance at $g = g_c = [\Delta(\delta_c^2 + \kappa^2)/(4\delta_c)]^{1/2}$ [37,38]. Superradiance is signaled by macroscopic coherences in the atomic medium $\langle\hat{X}^2\rangle \propto N^2$, $\hat{X} = \hat{b}_\uparrow^\dagger\hat{b}_\downarrow + \hat{b}_\downarrow^\dagger\hat{b}_\uparrow$, and a large cavity field $\langle\hat{a}^\dagger\hat{a}\rangle \propto N$. In this Letter, we focus on the subcritical regime to study the influence of time-periodic driving with $g(t) < g_c$ at all times. In this situation, a dynamical superradiant configuration can still be found depending on the modulation strength $g_1$ when the driving frequency $\omega$ is close to a parametric resonance [17], $n\omega = 2\omega_{\rm res}$ $(n = 1, 2, \dots)$ with resonance frequency

$$\omega_{\rm res} = \Delta\sqrt{1 - \frac{g_0^2}{g_c^2}}. \tag{3}$$

In Fig. 1 we show results for the time-averaged superradiance order parameter $\langle\hat{X}^2\rangle_{\rm tav} = \int_t^{t+T} d\tau\langle\hat{X}^2(\tau)\rangle/T$ as indicated by the color bar. The derivation of the phase transition lines of the superradiant region in the parameter space of $g_1$ and $\omega$ is given at a later point in this Letter. This superradiant phase features a time-oscillatory superradiant order parameter $\langle\hat{X}^2\rangle$. DTC order appears if additionally the two-time correlation function $C_1(t, t_0) = \langle\hat{X}(t + t_0)\hat{X}(t_0)\rangle$ is periodic in $t$ with period $2T$, $T = 2\pi/\omega$. This requires the breaking of a discrete time-translational symmetry which happens whenever $n$ is odd (see DTC in Fig. 1). The breaking of this symmetry implies the existence of a many-body mode oscillating with $\omega/2$ whose lifetime approaches infinity for increasing atom numbers. We remark that the driving sequence we employ is different from the one in Ref. [19], however, the consequences of breaking the time-translational symmetry are the same.

*Atom-only description*. First, we will derive the atom-only description, by extending the theory of Ref. [16] and applying it to a time-dependent problem. In the limit of a short cavity relaxation time, $|\delta_c - i\kappa| \gg \Delta, \omega, g$, we apply a Schrieffer-Wolff transformation $\hat{D}(t) = \exp[\hat{a}^\dagger\hat{\beta}(t) - \hat{\beta}^\dagger(t)\hat{a}]$ to eliminate the photonic degrees of freedom. The condition for decoupling the atoms from the cavity modes in the master equation leads to a *time-dependent* equation of the transformation operators $\hat{\beta}(t)$,

$$i\frac{\partial\hat{\beta}}{\partial t} = (\delta_c - i\kappa)\hat{\beta} + \frac{g(t)}{\sqrt{N}}(\hat{b}_\uparrow^\dagger\hat{b}_\downarrow + \hat{b}_\downarrow^\dagger\hat{b}_\uparrow) + [\Delta\hat{n}_\uparrow, \hat{\beta}], \tag{4}$$

which is solved by $\hat{\beta}(t) = c_+(t)\hat{b}_\uparrow^\dagger\hat{b}_\downarrow + c_-(t)\hat{b}_\downarrow^\dagger\hat{b}_\uparrow$ in the steady state. It is one major ingredient of this theory that we also include the commutator with $\Delta\hat{n}_\uparrow$ that adds retardation effects due to the time evolution of the atoms. Without this term the dynamical stabilization of the atomic state is not possible. The resulting differential equation is discussed in the Supplemental Material (SM) [39], which yields an expansion

$$c_\pm(t) \approx -\frac{1}{\sqrt{N}}\left(\frac{g(t)}{\delta_c - i\kappa} + \frac{i\dot{g}(t)}{(\delta_c - i\kappa)^2} \mp \frac{\Delta\, g(t)}{(\delta_c - i\kappa)^2}\right), \tag{5}$$

where the first term corresponds to the quasistatic solution. With $\hat{\beta}$ we can then write the effective master equation for the atomic density operator $\hat{\rho}_{\rm at} = {\rm Tr}_{\rm cav}[\hat{D}^\dagger\hat{\rho}\hat{D}]$ by tracing over the cavity degrees of freedom

$$\frac{\partial\hat{\rho}_{\rm at}}{\partial t} = -i[\hat{H}_{\rm at}, \hat{\rho}_{\rm at}] - \kappa(\hat{\beta}^\dagger\hat{\beta}\hat{\rho}_{\rm at} + \hat{\rho}_{\rm at}\hat{\beta}^\dagger\hat{\beta} - 2\hat{\beta}\hat{\rho}_{\rm at}\hat{\beta}^\dagger). \tag{6}$$

This atom-only description includes the coherent time evolution of the atoms governed by the Hamiltonian

$$\hat{H}_{\rm at} = \Delta\hat{n}_\uparrow + \frac{g(t)}{2\sqrt{N}}(\hat{\beta}^\dagger[\hat{b}_\uparrow^\dagger\hat{b}_\downarrow + \hat{b}_\downarrow^\dagger\hat{b}_\uparrow] + {\rm H.c.}). \tag{7}$$

The nontrivial time dependence of $\hat{\beta}(t)$ therefore enters both the (i) cavity-mediated interactions in the second term of Eq. (7) and the (ii) cavity-generated dissipation proportional to $\kappa$ in Eq. (6). In the SM [39] we provide a comparison of the atom-cavity and atom-only theory described by Eqs. (1) and (6), respectively.

*Formation of a stable DTC*. The resulting atomic theory described by Eqs. (6) and (7) is a full quantum mechanical description of the dynamics of the atomic state, which is the main tool in this Letter. The massively reduced Liouville space dimension allows us to study spectral features of the time-crystalline phase for atom numbers that cannot be accessed with a full atom-cavity description. Given a time-periodic Liouvillian [i.e., the right-hand side of Eq. (6)] we can calculate the eigenmodes $\hat{\rho}_\lambda = e^{\lambda t}\hat{\varrho}_\lambda$ with a time-periodic $\hat{\varrho}_\lambda(t + T) = \hat{\varrho}_\lambda(t)$. The eigenvalues $\lambda$ have in general a negative or zero real part, ${\rm Re}(\lambda) \leqslant 0$, and because of the time periodicity their imaginary value ${\rm Im}(\lambda)$ can be chosen within an interval of length $\omega$. The emergence of DTC is marked by the breaking of a discrete time-translational symmetry. This

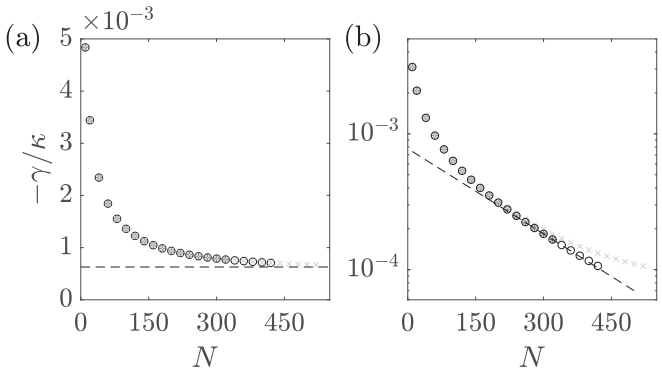


FIG. 2. Gap $\gamma$ in units of $\kappa$ as function of $N$ for (a) $g_1/g_0 = 0.05$ and (b) $g_1/g_0 = 0.2$. Different markers indicate different cutoffs in Floquet space (see SM [39], black circles $M_{\text{cut}} = 3$, gray stars $M_{\text{cut}} = 4$, light gray crosses $M_{\text{cut}} = 2$). The dashed line corresponds to (a) the mean-field $\gamma_{\text{Fl}}$ and (b) an exponential fit $\propto \exp(-0.005N)$.

results in a closing gap $\gamma := \text{Re}(\lambda)$ in the spectrum for increasing atom number $N$ at a subharmonic frequency response $\text{Im}(\lambda) = \omega/2$. The theory described by Eq. (6) enables the study of a decreasing $|\gamma|$ in the time-periodic Dicke model with only atomic degrees of freedom. In Figs. 2(a) and 2(b) we show $\gamma$ as a function of $N$ outside of the DTC phase (see the red cross in Fig. 1) in Fig. 2(a) and in the DTC phase (see the red star in Fig. 1) in Fig. 2(b). In Fig. 2(a) we find that $\gamma$ converges to a constant highlighting that this mode remains gapped. In Fig. 2(b), instead, we find an exponential closing of the gap therefore indicating time-crystalline behavior (further details in SM [39]). Our finding of an exponentially closing gap is consistent with previous claims [19] and enabled by our atom-only description that can access atom numbers in a range which is elusive for a full quantum atom-cavity description.

For very large atom numbers $N$ we can further simplify the full quantum description of the atom-only master equation to a mean-field description of $\varphi_s = \langle \hat{b}_s \rangle$, $s = \downarrow, \uparrow$ (see SM [39]),

$$\frac{d\varphi_\downarrow}{dt} = i\frac{V_0 - iV_1}{N}|\varphi_\uparrow|^2\varphi_\downarrow + i\frac{V_0 + iV_1}{N}\varphi_\uparrow^2\varphi_\downarrow^*, \tag{8}$$

$$\frac{d\varphi_\uparrow}{dt} = -i\left(\Delta - \frac{V_0 + iV_1}{N}|\varphi_\downarrow|^2\right)\varphi_\uparrow + i\frac{V_0 - iV_1}{N}\varphi_\downarrow^2\varphi_\uparrow^*. \tag{9}$$

This mean-field description includes (i) coherent interactions and (ii) dissipations that are described as nonlinear terms proportional to $V_0 = -\sqrt{N}g(t)\text{Re}(c_+ + c_-)$ and $V_1 = N\kappa(|c_-|^2 - |c_+|^2)$, respectively. The amplitude $c_-$ ($c_+$) describe the likelihood of atoms undergoing a transition from $|\uparrow\rangle$ to $|\downarrow\rangle$ ($|\downarrow\rangle$ to $|\uparrow\rangle$). Note that $V_1 \neq 0$ is a consequence of including retardation effects described by the commutator with $\Delta\hat{n}_\uparrow$ in Eq. (4). An imbalance, in our case $N(|c_-|^2 - |c_+|^2) = 4\delta_c\Delta g^2(t)/(\delta_c^2 + \kappa^2)^2 > 0$ for $\Delta, \delta_c > 0$, leads to a preferential reduction of atomic excitations. Consequently, dissipation described by $V_1$ has a nice physical interpretation: It is a cooling rate which is crucial for the stabilization of the system over long timescales. The efficient description given by Eqs. (8) and (9) allows us to map out the whole phase diagram visible in Fig. 1.

*Threshold.* We will now show that it is possible to derive analytical results for the onset of superradiance. We assume that all atoms are initially in the ground state and explore when driving induces an instability towards superradiance. With most bosons in $|\downarrow\rangle$, we eliminate fluctuations in the ground state using $\varphi_\downarrow \approx \sqrt{N}$, which linearizes Eq. (9). The resulting complex differential equation for $\boldsymbol{\varphi}_\uparrow = (\varphi_\uparrow, \varphi_\uparrow^*)$ can be solved using Floquet theory by making the ansatz $\boldsymbol{\varphi}_\uparrow(t) = e^{\lambda_{\text{Fl}}t}\mathbf{u}(t)$ with a $T = 2\pi/\omega$ periodic vector $\mathbf{u}$ and the Floquet eigenvalue $\lambda_{\text{Fl}} = \gamma_{\text{Fl}} - i\nu_{\text{Fl}}$, $\gamma_{\text{Fl}}, \nu_{\text{Fl}} \in \mathbb{R}$. Details of this derivation are reported in the SM [39]. The stability of the fluctuations is determined by $\gamma_{\text{max}}$ which is the maximum of all possible real parts $\gamma_{\text{Fl}}$. Whenever $\gamma_{\text{max}} \leqslant 0$ ($\gamma_{\text{max}} > 0$) we expect the system to be nonsuperradiant (superradiant). In the nonsuperradiant regime, the Floquet eigenvalues $\lambda_{\text{Fl}}$ represent the low-frequency modes $\lambda$ that are found using Floquet theory for the full Lindbladian in Eq. (6) for $N \to \infty$. To demonstrate this we show $\gamma_{\text{Fl}}$ as dashed line in Fig. 2(a) which appears to be the thermodynamic limit of $\gamma$. Above threshold, for $\gamma_{\text{Fl}} > 0$, such a comparison is not possible as $\lambda_{\text{FL}}$ can only describe the short-time dynamics. The threshold to superradiance is marked by $\gamma_{\text{Fl}} = 0$ and shown as a black line in Fig. 1. To get analytical expressions, we reformulate the coupled complex differential equation as a real second-order differential equation for $x_\uparrow = \varphi_\uparrow + \varphi_\uparrow^*$,

$$\frac{d^2x_\uparrow}{dt^2} + 2V_1(t)\frac{dx_\uparrow}{dt} + \Delta[\Delta - 2V_0(t)]x_\uparrow = 0. \tag{10}$$

In this differential equation $V_0$ modifies the resonance frequency $\Delta$ originating from (i) cavity-mediated interactions and $V_1$ serves as a damping of fluctuations coming from (ii) the cavity-generated dissipation. If we perform a first-order perturbation theory in $g_1/g_0 \sim \Delta/\sqrt{\delta_c^2 + \kappa^2}$, Eq. (10) becomes a Mathieu equation [40] with $V_1(t) \approx \gamma_0$ and $\Delta[\Delta - 2V_0(t)] \approx \omega_{\text{res}}^2 - 8\Delta\delta_c g_0 g_1/[\delta_c^2 + \kappa^2]\cos(\omega t)$. Here, we have introduced the time-independent damping

$$\gamma_0 = \frac{4\kappa\delta_c\Delta g_0^2}{\left[\delta_c^2 + \kappa^2\right]^2}, \tag{11}$$

and resonance frequency in Eq. (3). The Mathieu equation without damping is known to exhibit instabilities around the parametric resonances $n\omega = 2\omega_{\text{res}}$ [40]. In the presence of damping $\gamma_0$, instabilities require sufficiently strong driving, provided by the time-periodic term [40]. Accordingly, we observe in Fig. 1 superradiance close to the resonance condition $n\omega = 2\omega_{\text{res}}$ for pump power in the sidebands $\propto g_1/g_0$ above a certain threshold. This finding is in agreement with previous works where dynamical superradiance has been connected to the Mathieu equation [17,31], which again shows that the atomic quantum theory in Eq. (6) gives the correct behavior without describing explicitly the cavity. Moreover, this allows us to obtain simple results for the damping rate (11) and resonance frequency (3) and enables us to calculate the threshold in $g_1$. For this we perform a perturbative analysis around the first instability at $\omega = 2\omega_{\text{res}}$ reported in the SM [39]. We show that the instability occurs at

$$g_1^c = \frac{2\kappa\omega_{\text{res}}g_0}{\delta_c^2 + \kappa^2}. \tag{12}$$

The result given by Eq. (12) is visible as a gray solid line in Fig. 1. It agrees well with the threshold found using Floquet

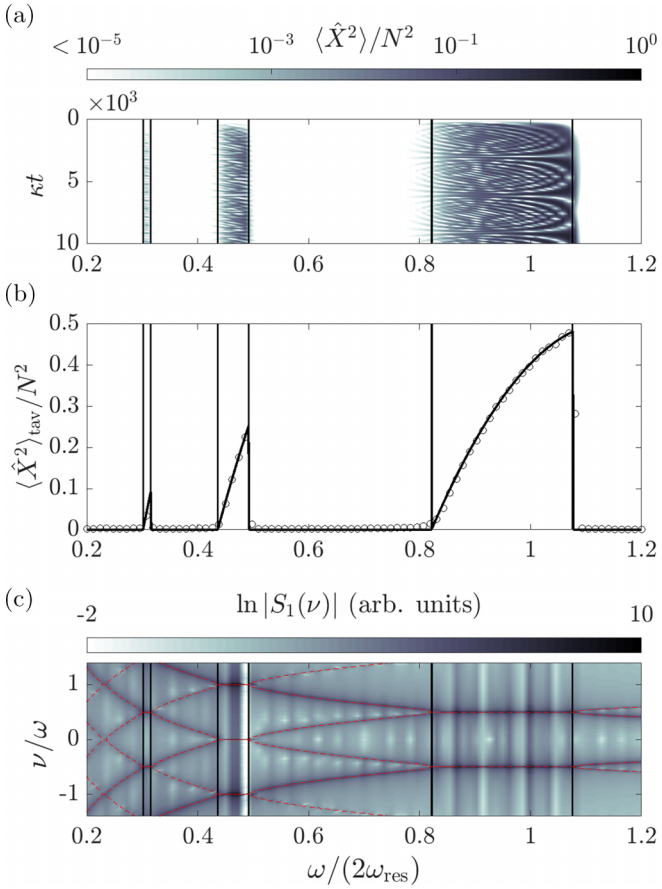


FIG. 3. (a) Superradiance order parameter $\langle \hat{X}^2 \rangle$ obtained from stochastic simulations as a function of time in units of $1/\kappa$ and of $\omega/(2\omega_{\rm res})$. The vertical black solid lines mark the threshold of superradiance obtained from the atom-only stability analysis. (b) Time-averaged superradiance order parameter $\langle \hat{X}^2 \rangle_{\rm tav}$ as a function of $\omega/(2\omega_{\rm res})$ evaluated after a time $\kappa t = 10^4$. Solid black lines (black circles) are obtained from the mean-field (semiclassical) simulations. (c) Spectrum $S_1(\nu)$ calculated from stochastic simulations as a function of $\nu/\omega$ and $\omega/(2\omega_{\rm res})$ with $\kappa t_0 = 5 \times 10^3$ and $t_{\rm max} = t_0$. The red dashed lines in (c) are $\nu_{\rm Fl}$. The remaining parameters are $\delta_c = \kappa$, $\Delta = 0.1\kappa$, $g_0 = 0.5 g_c$. The simulations are averaged over $10^4$ trajectories.

theory at $\omega = 2\omega_{\rm res}$ and its dependence on $\kappa$ highlights the effect of dissipation.

*Dynamical response of the atoms*. For a more comprehensive test of the atom-only theory and the resulting Floquet theory, we turn to semiclassical simulations of atoms and cavity (see SM [39]) for the same parameters as in Fig. 1, $g_1 = 0.75 g_0$, and different values of $\omega$ (the black dashed line in Fig. 1). For these parameters we expect three superradiant regimes around the parametric resonance $\omega = 2\omega_{\rm res}$, $2\omega = 2\omega_{\rm res}$, and $3\omega = 2\omega_{\rm res}$. We use the semiclassical simulations to calculate $\langle \hat{X}^2(t) \rangle$ shown as a function of time $t$ and driving frequency $\omega$ in Fig. 3(a). The atom-only theory predicts the borders of the superradiant regimes (black vertical lines), which fully agrees with large values $\langle \hat{X}^2 \rangle \propto N^2$. In Fig. 3(b), to compare the stationary state, we show the time-averaged superradiant order parameter $\langle \hat{X}^2 \rangle_{\rm tav}$ for both the semiclassical simulation of atoms and field (circles) and the atom-only mean-field theory (black solid line) at steady state. Both show a remarkable asymmetry of $\langle \hat{X}^2 \rangle_{\rm tav}$ where at each resonance the lower threshold to superradiance is a continuous transition while the upper threshold is marked by a sudden jump of $\langle \hat{X}^2 \rangle_{\rm tav}$. Our semiclassical simulations provide a powerful tool in its own right for studying the dynamics. The perfect quantitative agreement with the atom-only model demonstrates that the nontrivial microscopic derivation of an effective quantum damping mechanism can be used far from equilibrium. This agreement paves the way for studies of atomic quantum correlations and gaps as well as more involved time-dependent protocols with the full quantum model.

To understand the dynamical response of the atoms, which is crucial to determine whether one finds a subharmonic and time-crystalline order, we employ the two-time correlation function $C_1(t, t_0)$ and calculate its Fourier transform $S_1(\nu) = \int_0^{t_{\rm max}} dt e^{i\nu t} C_1(t, t_0)$. Here, $t_0$ is a long time after which the dynamics of the system becomes independent of its initial condition and $t_{\rm max}$ is a long-time cutoff. The numerical result of $S_1(\nu)$ is shown in Fig. 3(c) as a function of $\nu$ and driving frequency $\omega$. The spectrum $S_1(\nu)$ spikes in $\nu$ for all values of $\omega$ that highlight resonances in the atomic medium. These resonances are in agreement with the Floquet frequencies $\nu_{\rm Fl}$ that are visible as red dashed lines in Fig. 3(c). We find $\nu_{\rm Fl} = n\omega/2$ in the dynamical superradiant phase corresponding to the parametric resonance $n\omega = 2\omega_{\rm res}$. This implies that the response of the atoms is flat with respect to the driving frequency which highlights its robustness. Moreover, the response is subharmonic whenever $n$ is odd, which becomes clear when considering that the underlying model is a single-mode theory of $\varphi_\uparrow$ that oscillates with $\omega_{\rm res} = n\omega/2$.

*Conclusions*. In conclusion, we have derived and verified an atom-only theory for the time-periodic dissipative Dicke model. With this theory we studied the onset of superradiance including the dynamical response and the threshold determined by the cavity-generated dissipation, the driving frequency, and amplitude. Besides the numerical efficiency and maybe most remarkably, this atom-only theory allows us also to describe the long-time relaxation into the DTC that we can understand from an effective cooling mechanism. We remark that all studied quantities in this Letter including the superradiance order parameter and spectrum can be measured from the cavity output. Future theoretical avenues that build on the presented theory could use the atom-only theory to derive quantum fluctuations and low-energy excitations of the DTC. This can be used to determine if the emergent states are quantum entangled [41]. In addition, one can apply the atom-only theory to more complicated systems with many and eventually infinitely many cavity modes. This paves the way to the efficient theoretical description of the atomic medium under periodic driving, which can be used to analyze the generation of squeezed and entangled atomic states with quantum information and metrology applications [42,43].

*Acknowledgments*. S.B.J. acknowledges stimulating discussions with A. Pelster, R. Betzholz, G. Morigi, J. Reilly, and M. J. Holland. We acknowledge support from Research Centers of the Deutsche Forschungsgemeinschaft (DFG, German Research Foundation) Project No. 277625399-TRR 185 OSCAR (A4,A5).

[1] J. Dalibard, F. Gerbier, G. Juzeliūnas, and P. Öhberg, *Colloquium*: Artificial gauge potentials for neutral atoms, Rev. Mod. Phys. **83**, 1523 (2011).

[2] K. Wintersperger, C. Braun, F. N. Ünal, A. Eckardt, M. D. Liberto, N. Goldman, I. Bloch, and M. Aidelsburger, Realization of an anomalous Floquet topological system with ultracold atoms, Nat. Phys. **16**, 1058 (2020).

[3] K. Staliunas, S. Longhi, and G. J. de Valcárcel, Faraday patterns in Bose-Einstein condensates, Phys. Rev. Lett. **89**, 210406 (2002).

[4] C. Chin, R. Grimm, P. Julienne, and E. Tiesinga, Feshbach resonances in ultracold gases, Rev. Mod. Phys. **82**, 1225 (2010).

[5] A. M. Perego, N. Tarasov, D. V. Churkin, S. K. Turitsyn, and K. Staliunas, Pattern generation by dissipative parametric instability, Phys. Rev. Lett. **116**, 028701 (2016).

[6] L. W. Clark, A. Gaj, L. Feng, and C. Chin, Collective emission of matter-wave jets from driven Bose–Einstein condensates, Nature (London) **551**, 356 (2017).

[7] J. H. V. Nguyen, M. C. Tsatsos, D. Luo, A. U. J. Lode, G. D. Telles, V. S. Bagnato, and R. G. Hulet, Parametric excitation of a Bose-Einstein condensate: From Faraday waves to granulation, Phys. Rev. X **9**, 011052 (2019).

[8] Z. Zhang, K.-X. Yao, L. Feng, J. Hu, and C. Chin, Pattern formation in a driven Bose–Einstein condensate, Nat. Phys. **16**, 652 (2020).

[9] S. Fazzini, P. Chudzinski, C. Dauer, I. Schneider, and S. Eggert, Nonequilibrium Floquet steady states of time-periodic driven Luttinger liquids, Phys. Rev. Lett. **126**, 243401 (2021).

[10] A. Eckardt, *Colloquium*: Atomic quantum gases in periodically driven optical lattices, Rev. Mod. Phys. **89**, 011004 (2017).

[11] C. Weitenberg and J. Simonet, Tailoring quantum gases by Floquet engineering, Nat. Phys. **17**, 1342 (2021).

[12] F. Petiziol and A. Eckardt, Cavity-based reservoir engineering for Floquet-engineered superconducting circuits, Phys. Rev. Lett. **129**, 233601 (2022).

[13] B. Zhu, J. Marino, N. Y. Yao, M. D. Lukin, and E. A. Demler, Dicke time crystals in driven-dissipative quantum many-body systems, New J. Phys. **21**, 073028 (2019).

[14] F. Damanet, A. J. Daley, and J. Keeling, Atom-only descriptions of the driven-dissipative Dicke model, Phys. Rev. A **99**, 033845 (2019).

[15] A. V. Bezvershenko, C.-M. Halati, A. Sheikhan, C. Kollath, and A. Rosch, Dicke transition in open many-body systems determined by fluctuation effects, Phys. Rev. Lett. **127**, 173606 (2021).

[16] S. B. Jäger, T. Schmit, G. Morigi, M. J. Holland, and R. Betzholz, Lindblad master equations for quantum systems coupled to dissipative bosonic modes, Phys. Rev. Lett. **129**, 063601 (2022).

[17] R. Chitra and O. Zilberberg, Dynamical many-body phases of the parametrically driven, dissipative Dicke model, Phys. Rev. A **92**, 023815 (2015).

[18] F. Iemini, A. Russomanno, J. Keeling, M. Schirò, M. Dalmonte, and R. Fazio, Boundary time crystals, Phys. Rev. Lett. **121**, 035301 (2018).

[19] Z. Gong, R. Hamazaki, and M. Ueda, Discrete time-crystalline order in cavity and circuit QED systems, Phys. Rev. Lett. **120**, 040404 (2018).

[20] H. Keßler, P. Kongkhambut, C. Georges, L. Mathey, J. G. Cosme, and A. Hemmerich, Observation of a dissipative time crystal, Phys. Rev. Lett. **127**, 043602 (2021).

[21] P. Kongkhambut, H. Keßler, J. Skulte, L. Mathey, J. G. Cosme, and A. Hemmerich, Realization of a periodically driven open three-level Dicke model, Phys. Rev. Lett. **127**, 253601 (2021).

[22] P. Kongkhambut, J. Skulte, L. Mathey, J. G. Cosme, A. Hemmerich, and H. Keßler, Observation of a continuous time crystal, Science **377**, 670 (2022).

[23] A. Kosior, H. Ritsch, and F. Mivehvar, Nonequilibrium phases of ultracold bosons with cavity-induced dynamic gauge fields, SciPost Phys. **15**, 046 (2023).

[24] X. Nie and W. Zheng, Mode softening in time-crystalline transitions of open quantum systems, Phys. Rev. A **107**, 033311 (2023).

[25] J. B. Curtis, Z. M. Raines, A. A. Allocca, M. Hafezi, and V. M. Galitski, Cavity quantum Eliashberg enhancement of superconductivity, Phys. Rev. Lett. **122**, 167002 (2019).

[26] R. Palacino and J. Keeling, Atom-only theories for U(1) symmetric cavity-QED models, Phys. Rev. Res. **3**, L032016 (2021).

[27] S. P. Kelly, J. K. Thompson, A. M. Rey, and J. Marino, Resonant light enhances phase coherence in a cavity QED simulator of fermionic superfluidity, Phys. Rev. Res. **4**, L042032 (2022).

[28] H. Ritsch, P. Domokos, F. Brennecke, and T. Esslinger, Cold atoms in cavity-generated dynamical optical potentials, Rev. Mod. Phys. **85**, 553 (2013).

[29] F. Mivehvar, F. Piazza, T. Donner, and H. Ritsch, Cavity QED with quantum gases: new paradigms in many-body physics, Adv. Phys. **70**, 1 (2021).

[30] N. Defenu, T. Donner, T. Macrì, G. Pagano, S. Ruffo, and A. Trombettoni, Long-range interacting quantum systems, Rev. Mod. Phys. **95**, 035002 (2023).

[31] P. Molignini, L. Papariello, A. U. J. Lode, and R. Chitra, Superlattice switching from parametric instabilities in a driven-dissipative Bose-Einstein condensate in a cavity, Phys. Rev. A **98**, 053620 (2018).

[32] J. G. Cosme, J. Skulte, and L. Mathey, Time crystals in a shaken atom-cavity system, Phys. Rev. A **100**, 053615 (2019).

[33] J. G. Cosme, J. Skulte, and L. Mathey, Bridging closed and dissipative discrete time crystals in spin systems with infinite-range interactions, Phys. Rev. B **108**, 024302 (2023).

[34] F. Dimer, B. Estienne, A. S. Parkins, and H. J. Carmichael, Proposed realization of the Dicke-model quantum phase transition in an optical cavity QED system, Phys. Rev. A **75**, 013804 (2007).

[35] K. Baumann, C. Guerlin, F. Brennecke, and T. Esslinger, Dicke quantum phase transition with a superfluid gas in an optical cavity, Nature (London) **464**, 1301 (2010).

[36] J. Larson and T. Mavrogordatos, *The Jaynes–Cummings Model and Its Descendants* (IOP Publishing, Bristol, UK, 2021).

[37] E. G. D. Torre, S. Diehl, M. D. Lukin, S. Sachdev, and P. Strack, Keldysh approach for nonequilibrium phase transitions in quantum optics: Beyond the Dicke model in optical cavities, Phys. Rev. A **87**, 023831 (2013).

[38] P. Kirton, M. M. Roses, J. Keeling, and E. G. D. Torre, Introduction to the Dicke model: From equilibrium to nonequilibrium, and vice versa, Adv. Quantum Technol. **2**, 1800043 (2019).

[39] See Supplemental Material at http://link.aps.org/supplemental/10.1103/PhysRevA.110.L010202 for more details, which includes Refs. [44,45].

[40] I. Kovacic, R. Rand, and S. M. Sah, Mathieu's equation and its generalizations: Overview of stability charts and their features, Appl. Mech. Rev. **70**, 020802 (2018).

[41] R. Mattes, I. Lesanovsky, and F. Carollo, Entangled time-crystal phase in an open quantum light-matter system, Phys. Rev. A **108**, 062216 (2023).

[42] J. T. Reilly, S. B. Jäger, J. D. Wilson, J. Cooper, S. Eggert, and M. J. Holland, Speeding up squeezing with a periodically driven Dicke model, arXiv:2310.07694.

[43] C. Luo, H. Zhang, A. Chu, C. Maruko, A. M. Rey, and J. K. Thompson, Hamiltonian engineering of collective XYZ spin models in an optical cavity: From one-axis twisting to two-axis counter twisting models, arXiv:2402.19429.

[44] J. H. Taylor and K. S. Narendra, Stability regions for the damped Mathieu equation, SIAM J. Appl. Math. **17**, 343 (1969).

[45] P. Domokos, P. Horak, and H. Ritsch, Semiclassical theory of cavity-assisted atom cooling, J. Phys. B: Mol. Opt. Phys. **34**, 187 (2001).